



Upregulation of histone H3 caused by CRYAA may contribute to the development of age-related cataract

CHAO WANG^{1,2}; JUNWEI WANG¹; FANQIAN SONG^{1,2}; HANRUO LIU³; LIYAO SUN^{1,2}; XI WEI^{1,2}; TAO ZHENG¹; HUA QIAN²; XIAOGUANG LI²; WEIHUA ZHANG⁴; XIANLING TANG^{1,*}; PING LIU^{1,*}

¹ Eye Hospital, First Affiliated Hospital, Harbin Medical University, Harbin, 150001, China

² Department of Pharmacology, College of Pharmacy, Harbin Medical University, and Heilongjiang Academy of Medical Sciences, Harbin, 150081, China

³ Beijing Institute of Ophthalmology, Beijing Tongren Hospital, Capital Medical University, Beijing Ophthalmology & Visual Science Key Lab, Beijing, 100000, China

⁴ Department of Pathophysiology, Harbin Medical University, Harbin, 150081, China

Key words: Age-related cataract, Histone H3, α A-crystallin, Anterior lens capsules, Basement membrane

Abstract: Objective: Age-related cataract (ARC) is a disease of the eyes with no effective drugs to prevent or treat patients. The aim of the present study is to determine whether histone H3, α A-crystallin (CRYAA), β -galactosidase (GLB1), and p53 are involved in the pathogenesis of ARC. **Methods:** A total of 99 anterior lens capsules (ALCs) of patients with ARC of various nuclear grades, ultraviolet models of ALCs, and two human lens epithelial cell lines (FHL-124 and SRA01/04) were used, and the expression of histone H3, CRYAA, GLB1, and p53 were detected by immunoblotting and reverse transcription and real time-quantitative polymerase chain reaction. The association between CRYAA with histone H3, GLB1, and p53 was assessed in FHL-124 and SRA01/04 cells following CRYAA overexpression. **Results:** Histone H3 and p53 in ALCs of patients with ARC were up-regulated in a grade-dependent manner, and the expression of CRYAA showed a positive association with histone H3, p53, and GLB1. In UV models of ALCs and human lens epithelial cell lines, the expression levels of histone H3, cell apoptosis factors (Bax/Bcl-2, cleaved caspase-3), and inflammation factors (interleukin-6, tumor necrosis factor- α) were all up-regulated. Furthermore, transfection of CRYAA in FHL-124 cells induced overexpression of histone H3. **Conclusion:** CRYAA-mediated upregulation of histone H3 may be involved in the pathogenesis of ARC. p53 may also have a role in ARC development, but not via the CRYAA-histone H3 axis. The results of the present study may assist in improving our understanding of the pathogenesis of ARC and in identifying potential targets for treatment.

Abbreviations

ALCs:	anterior lens capsules
ARC:	age-related cataract
BM:	basement membrane
CRYAA:	α A-crystallin
GLB1:	β -galactosidase
IB:	immunoblotting
IL-6:	interleukin-6
mAb:	monoclonal antibody
pAb:	polyclonal antibody
PBS:	phosphate buffered saline
RT-qPCR:	reverse transcription-quantitative polymerase chain reaction

TNF- α : tumor necrosis factor- α

UV: ultraviolet

Introduction

Cataract is one of the major causes of blindness and vision impairment worldwide, particularly in developing countries (Flaxman *et al.*, 2017; Khairallah *et al.*, 2015). Although visual function can be restored by surgery for cataracts, there are currently no effective drugs to prevent or treat cataract. Studying the pathogenesis of cataracts for the identification of novel therapeutic targets may assist in the need for surgery. Several risk factors, such as aging, genetic factors, traumatic injury, other ocular or systemic disease, endocrine disease, use of drugs or toxins, irradiation, poor nutrition, alcohol abuse, and smoking, may cause cataract (Nizami and Gulani, 2021). According to the etiology, cataract is classified as age-related cataract (ARC), childhood cataract, traumatic cataract, cataract

*Address correspondence to: Ping Liu, liuping2017lq@163.com; Xianling Tang, tangxianling@163.com
Received: 04 May 2022; Accepted: 12 July 2022



associated with systemic disease, complicated cataract, and drug-induced cataract, among which ARC was the most common type (Richard, 2019).

ARC is further classified into nuclear cataracts, cortical cataracts, and posterior subcapsular cataracts, among which nuclear cataracts are the most common (Thompson and Lakhani, 2015; Klein et al., 2002; Tang et al., 2016). Both genetic and environmental factors are important in the development of ARC (Hammond et al., 2000). Damage to human lens epithelial cells, caused by cell apoptosis, senescence, or pyroptosis, is one of the major pathological bases of this disease (Li et al., 1995; Fu et al., 2016; Jin et al., 2017). ARC is caused by oxidative stress, and in particular, age-related nuclear cataract (Vinson, 2006; Beebe et al., 2010), and ultraviolet (UV) irradiation increases oxidative stress in human lens epithelial cells (Yao et al., 2008). In addition, UV irradiation may induce aggregation of α , β and γ crystallin protein mixtures, which are also the pathological basis of ARC (Pitts et al., 1977). The insolubility of crystallin proteins and the formation of large protein aggregates increase with the nuclear grades of ARC (Truscott, 2005).

The major aim of our studies was to study the contribution of proteins in human anterior lens capsules (ALCs) to the pathogenesis of ARC. In our previous study, the expression of laminin $\alpha 4$, $\beta 2$, $\gamma 1$ subunits was shown to be positive in the basement membrane (BM) of a human lens epithelial cell line, HLE B-3; and laminin $\alpha 4$, $\gamma 1$, and $\gamma 2$ was detected in human ALCs, suggesting that HLE B-3 cells may produce an anterior-capsule-like BM with rich laminins *in vitro*, which could be used to study the role of laminins in ALCs in the pathogenesis of lens diseases, particularly cataracts (Yan et al., 2018). In another previous study from our lab, a positive association was observed between the expression levels of p53 and total laminin in cataractous ALCs, and both increased with the nuclear grade of ARC. These results suggest that both p53 and laminins may be involved in the pathogenesis of ARC, and the expression levels of p53 and total laminin in cataractous ALCs may be used as markers for severities of ARC (Yan et al., 2019).

In the present study, 99 ALC samples from patients of ARC with various nuclear grades were used for the analysis of the expressions of histone H3, CRYAA, GLB1, and p53 by immunoblotting (IB) and to determine their association with the nuclear grades of ARC. Furthermore, UV models using ALCs and two human lens epithelial cell lines, FHL-124 and SRA01/04, were used to confirm whether these factors participate in the pathogenesis of ARC. Finally, the possible regulatory association between CRYAA and the other three factors was preliminarily studied *in vitro* in FHL-124 and SRA01/04.

Materials and Methods

Collection of human ALCs

Human ALC samples obtained from 99 eyes (99 patients) with age-related nuclear cataract (mean age \pm standard deviation, 67.5 ± 10.44 , age range, 50–97 years old; 35 males, 64 females) were collected in 2021–2022 at the First Affiliated Hospital of Harbin Medical University. Human ALCs were obtained by a single ophthalmologist using the central circular capsulorhexis method from the anterior surface of the cataractous lens during

surgery of patients with cataracts (Andjelic et al., 2017); ALC samples were kept at -80°C . All patients were free of other ocular diseases and were graded for cataract severity by the Emery-Little Classification System of nuclear opacity grade before surgery (Zeng et al., 2008; Ikeda et al., 2014). All experiments were approved by the Internal Review Board of Harbin Medical University and were performed in accordance with the Declaration of Helsinki Principles. Informed consent was obtained from each patient.

ALC culture

Human ALC samples with human lens epithelial cells were dissected from the cataractous lens and maintained in Dulbecco's modified Eagle medium (DMEM; Hyclone; GE Healthcare Life Sciences, Logan, UT, USA) containing 10% fetal bovine serum (Gibco; Thermo Fisher Scientific, Inc., Waltham, MA, USA), 100 U/mL penicillin and 100 $\mu\text{g}/\text{mL}$ streptomycin (Beyotime Biotechnology, Shanghai, China) at 37°C overnight for the subsequent next UV irradiation experiments, or lysed with cold radioimmunoprecipitation assay buffer as described previously (Yan et al., 2019).

Human lens epithelial cells

The human lens epithelial cell lines (FHL-124 cells and SRA01/04 cells) were purchased from the American Type Culture Collection (Manassas, VA, USA). Cell culture and supernatants, cell lysates, and BMs were collected as described previously (Yan et al., 2018; Yan et al., 2019). After the collection of cell lysate, the dishes were washed with PBS twice, and the dish was visualized under a microscope to ensure no cells were left. Subsequently, 1000 μL of $2 \times$ loading buffer was added to the dish, and the bottom of the dish was scraped using a cell scraper firmly for 2 min. Finally, the loading buffer containing BM proteins was collected and stored at -20°C for further experiments.

UV irradiation experiment

ALCs of nuclear grade 2 were first plated in a 35-mm dish containing 750 μL phosphate-buffered saline (PBS) and were treated with UV ($100 \mu\text{W}/\text{cm}^2$) for 30 min. Subsequently, the PBS in each dish was replaced with 1.5 ml fresh low-glucose DMEM containing 10% fetal bovine serum, 100 units/mL penicillin, 100 $\mu\text{g}/\text{mL}$ streptomycin, and the ALCs were cultured at 37°C with 5% CO_2 . After 24 h of incubation, ALCs were treated with UV for 1 h as described above, and the lysates of ALCs were then prepared as described previously (Yan et al., 2019).

For the UV irradiation experiment of cells, FHL-124 cells and SRA01/04 cells were seeded in 10 cm dishes and grown to a confluency of 95%. After discarding the culture supernatant, cells were washed twice with PBS, and finally, 3 mL PBS was added to each dish. Cells were then treated with UV ($100 \mu\text{W}/\text{cm}^2$) for 1 h, and control cells were kept at room temperature without UV irradiation for 1 h. After irradiation, the supernatant (PBS), lysate, and BM were then collected. The collected supernatant (PBS) of cells was centrifuged at $3000 \times g$ for 2 min at 4°C , and the supernatant was concentrated using an Amicon Ultra-0.5 (EMD Millipore), according to the manufacturer's protocol.

Plasmid construction and cell transfection

The pcDNA3.1(+)-CRYAA plasmid was constructed as described previously (18). Cell transfection of CRYAA plasmid

with pcDNA3.1(+) blank vector as the negative control were performed as previously described (Yu *et al.*, 2019).

Antibodies

The antibodies used in the present study were: Mouse monoclonal antibody (mAb) against histone H3 (1:1000, cat no. AF0009; Beyotime Biotechnology, Shanghai, China), mouse mAb against β -actin (1:1000, cat no. TA-09; ZSGB-BIO, Beijing, China), rabbit polyclonal antibody (pAb) against CRYAA (1:1000, cat no. abs116815; Absin Bioscience, Shanghai, China), rabbit pAb against p53 (1:2000, cat no. B0530; AssayBiotech, Fremont, CA, USA), rabbit mAb against beta-galactosidase (GLB1) (1:10000, cat no. ab128993; Abcam, England), rabbit mAb against caspase-3 (1:1000, cat no. #14220; Cell Signaling Technology, Inc., Danvers, MA, USA), rabbit pAb against Bcl-2 (1:1000, cat no. B0774; AssayBiotech, Fremont, CA, USA), rabbit pAb against Bax (1:10000, cat no. B0773; ProteinTech Group, Inc., Rosemont, IL, USA), rabbit mAb against phospho-(p)-histone H3(1:500, cat no. AF1180; Beyotime Biotechnology, Shanghai, China).

Bicinchoninic acid assay

A bicinchoninic acid assay kit (Beyotime Biotechnology, Shanghai, China) was used to detect protein concentrations of ALCs and human lens epithelial cells according to the manufacturer's protocol.

Immunoblotting

Protein levels in human ALC lysate, in the supernatant, lysate, and BMs of FHL-124 cells and SRA01/04 cells were analyzed by IB as described previously (Yan *et al.*, 2018; Yan *et al.*, 2019). As an internal control of BMs, Coomassie brilliant blue (CBB) staining was used instead of β -actin, which could not be detected in BMs.

CBB staining assay

CBB staining assay was performed as described previously (Yan *et al.*, 2019).

Reverse transcription and reverse transcription-quantitative polymerase chain reaction (RT-qPCR)

Total following UV irradiation and transfection of CRYAA plasmid, RNA of human lens epithelial cells was isolated with TRIZOL reagent (HaiGene, Harbin, Heilongjiang, China) according to the manufacturer's protocol. cDNA was reverse transcribed from total RNA with the ReverTra Ace[®] qPCR RT Kit (Toyobo Life Science, Osaka, Japan). Fluorescent RT-qPCR was performed using special gene primers and the SYBR[®] Green Realtime PCR Master Mix (Toyobo Life Science, Osaka, Japan) in an ABI QuantStudio 6 Flex Real-Time PCR System (Thermo Fisher Scientific Inc., Waltham, Massachusetts, USA). The amplification conditions consisted of an initial step of denaturation at 95°C for 1 min, followed by denaturation at 95°C for 15 s, 40 cycles and annealing at 55°C for 15 s and extension at 72°C for 1 min, and a final 72°C for 1 min. β -actin was used as the internal control. The expression level of each gene was represented as the fold change using the $2^{-\Delta\Delta C_t}$ method. Relative expression of each gene was shown with that of cells without treatment as control. The primers used are listed in Table 1.

Statistical analysis

Statistical analysis was performed using SigmaPlot 12.0 (Hulinks, Inc., Tokyo, Japan). Pearson correlation coefficient analysis, Kruskal-Wallis test with Dunn's post-hoc test, and ANOVA were used to analyze the differences between experimental groups. $p < 0.05$ was considered to indicate a statistically significant difference.

Results

Clinical characters of patients with age-related cataract

In the present study, ALCs from 99 patients with ARC were collected and categorized into three groups according to the nuclear grade of cataract: Grade 2, $n = 34$; grade 3, $n = 38$; and grade 4+ (grade 4 and grade 5), $n = 27$. The age, sex, and ARC nuclear grade of all patients involved in the present study are summarized in Table 2. The ages of ARC patients with grade 4+ ($p < 0.05$) and grade 3 ($p < 0.05$) were significantly higher compared with those with grade 2; there was no significant difference between the age of patients with grade 4+ or grade 3 ARC (Fig. 1). There was no significant difference in the age and nuclear grade between male and female patients (data not shown).

Detection of histone H3, p53, β -galactosidase, and α A-crystallin, in anterior lens capsules of age-related cataract IB assays showed that most of the ALCs from patients were shown to express histone H3, p53, GLB1, and CRYAA (Fig. 2a). Quantitative analysis of the IB results showed that the expression levels of histone H3 in ALCs of grade 4+ were

TABLE 1

The primer sequences for reverse transcription-quantitative polymerase chain reaction

Gene	Primer sequence
Bax-F	5'-TTGCTTCAGGGTTTCATCCA-3'
Bax-R	5'-CAGCCTTGAGCACCAGTTTG-3'
Bcl2-F	5'-GTGGAGGAGCTCTTCAGGGA-3'
Bcl2-R	5'-AGGCACCCAGGGTGATGCAA-3'
IL-6-F	5'-ATGAACTCCTTCTCCACAAG-3'
IL-6-R	5'-GTGCCTGCAGCTTCGTGAGCA-3'
TNF- α -F	5'-TCAGATCATCTTCTCGAACC-3'
TNF- α -R	5'-CAGATAGATGGGCTCATAACC-3'
Histone H3-F	5'-ACTGCTCGGAAGTCTACTGGT-3'
Histone H3-R	5'-GCGCTGGAAAGGTAGTTTACGA-3'
p53-F	5'-GACGGAGGTTGTGAGGCG-3'
p53-R	5'-CAGTGTGATGATGGTGAGGATG-3'
p21-F	5'-CGTGAGCGATGGAACCTCGA-3'
p21-R	5'-CTCTTGAGAGAAGATCAGCCG-3'
CRYAA-F	5'-TTTTGAGTATGACCTGCTGCC-3'
CRYAA-R	5'-CAGAAGGTCAGCATGCCATC-3'
β -actin-F	5'-TGACGGGGTCACCCACACTGTGCCCATCTA-3'
β -actin-R	5'-CTAGAAGCATTTGCGGTGGACGATGGAGGG-3'

TABLE 2

Clinical information of patients with age-related cataract

No.	Sex	Age	Grade
1	female	47	2
2	male	48	2
3	male	49	2
4	female	49	2
5	male	49	2
6	male	49	2
7	female	54	2
8	female	55	2
9	male	55	2
10	male	58	2
11	female	59	2
12	female	61	2
13	female	61	2
14	female	61	2
15	male	61	2
16	female	62	2
17	female	62	2
18	female	62	2
19	female	63	2
20	female	63	2
21	female	63	2
22	male	67	2
23	female	68	2
24	male	69	2
25	female	69	2
26	male	71	2
27	female	72	2
28	male	72	2
29	male	72	2
30	female	73	2
31	female	76	2
32	female	77	2
33	female	81	2
34	female	85	2
35	male	81	3
36	female	80	3
37	male	79	3
38	male	75	3
39	male	74	3
40	female	73	3
41	female	72	3
42	female	64	3
43	female	63	3
44	male	56	3
45	male	54	3

(Continued)

Table 2 (continued)

No.	Sex	Age	Grade
46	female	50	3
47	male	50	3
48	male	68	3
49	male	unknown	3
50	male	71	3
51	male	66	3
52	female	79	3
53	female	76	3
54	female	64	3
55	male	73	3
56	female	63	3
57	female	80	3
58	female	49	3
59	female	66	3
60	female	75	3
61	female	59	3
62	unknown	unknown	3
63	female	78	3
64	female	75	3
65	male	76	3
66	female	63	3
67	female	77	3
68	male	53	3
69	male	87	3
70	female	78	3
71	male	77	3
72	male	59	3
73	female	86	4
74	female	84	4
75	male	78	4
76	female	78	4
77	female	76	4
78	female	73	4
79	female	71	4
80	male	69	4
81	male	64	4
82	unknown	unknown	4
83	male	61	4
84	unknown	unknown	4
85	female	65	4
86	female	84	4
87	female	60	4
88	female	79	4
89	male	50	4
90	female	65	4
91	female	unknown	4
92	female	82	4

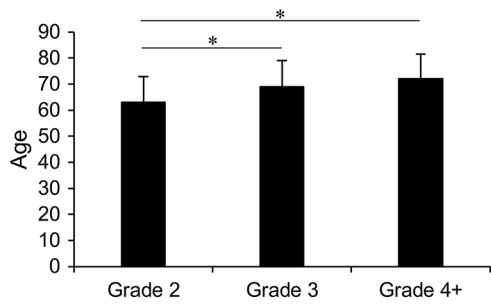


FIGURE 1. Correlation between patient age and ARC nuclear opacity grade. A total of 99 ALCs from patients with ARC were collected and categorized into three groups: Grade 2 (n = 34), grade 3 (n = 38), and grade 4+ (grades 4 and 5, n = 27). Data were shown as mean ± SD and were analyzed using Kruskal-Wallis test with Dunn's post-hoc test. *, $p < 0.05$. ARC, age-related cataracts; ALC, anterior lens capsules.

significantly higher compared with grade 2 ($p < 0.05$; Fig. 2b), there was no significant difference in the expression levels of histone H3 in ALCs between grade 3 and grade 2 or grade 4+. The expression levels of p53 in ALCs of grade 4+ ($p < 0.05$) and grade 3 ($p < 0.05$) patients were significantly higher compared with grade 2 patients (Fig. 2c). There was no significant difference in the expression levels of GLB1 (Fig. 2d) and CRYAA (Fig. 2e) in ALCs between the three groups.

Correlation between histone H3, p53, β-galactosidase, and αA-crystallin, in anterior lens capsules of age-related cataract
The correlation between histone H3, p53, GLB1, and CRYAA in ALCs was analyzed based on densitometry analysis of the IB results, and significant data are summarized in Fig. 3. In the total of 99 ALC samples, the levels of CRYAA were positively correlated with those of histone H3 ($R = 0.494$, $p < 0.001$; Fig. 3a), p53 ($R = 0.382$, $p < 0.001$; Fig. 3b), and GLB1 ($R = 0.464$, $p < 0.001$; Fig. 3c). The levels of GLB1 were positively correlated with those of p53 ($R = 0.669$,

$p < 0.001$; Fig. 3d). In addition, the age and sex of the patients with ARC were not significantly correlated with the levels of histone H3, p53, GLB1, and CRYAA in ALCs (data not shown).

Histone H3, p-histone H3, p53, β-galactosidase, and αA-crystallin, in anterior lens capsules of age-related cataract after UV irradiation

An *in vitro* ARC model was established using grade 2 ALCs treated with UV irradiation. After UV irradiation, human lens epithelial cells in ALCs became swollen (Fig. 4a). CBB staining of the lysates of ALCs was used to confirm the loaded equivalent dose (Fig. 4b). The expression of p53 and GLB1 was not detectable by IB in both UV-treated and untreated ALCs (Fig. 4b). Compared with the untreated ALCs, UV-treated ALCs showed higher levels of histone H3 ($p < 0.001$; Figs. 4b and 4c), and lower levels of CRYAA ($p < 0.05$; Figs. 4b and 4d) and p-histone H3 (Fig. 4b).

Histone H3, p-histone H3, p53, β-galactosidase, and αA-crystallin in the supernatant, lysate and basement membrane of SRA04/01 cells treated with UV irradiation

UV irradiation induces cell trauma, which can be used as a model of ARC (15). In the present study, SRA01/04 cells were treated with UV irradiation for 1 h, and then the supernatant, lysate, and BM were harvested and analyzed by IB to detect the expression of histone H3, p-histone H3, p53, GLB1, and CRYAA. Total RNA was collected, and levels of mRNAs coding for Bcl-2, Bax, interleukin-6 (IL-6), tumor necrosis factor-α (TNF-α), histone H3, p53, CRYAA, and p21 were detected by RT-qPCR. After UV irradiation, SRA01/04 cells showed shrinking, budding and apoptotic-like characteristics (Fig. 5a). UV-induced cell apoptosis was further confirmed by increased Bax, cleaved caspase-3, and decreased Bcl-2 expression by IB (Fig. 5b), and increased mRNA levels of Bax ($p < 0.05$) by RT-qPCR (Fig. 5c). In addition, following UV

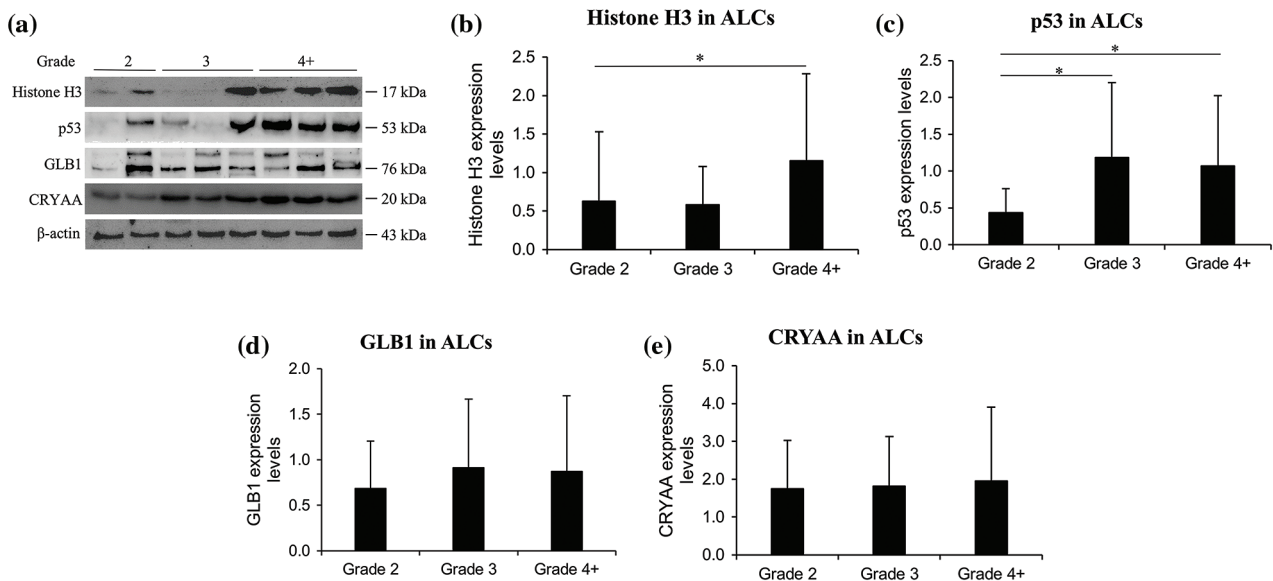


FIGURE 2. Histone H3, p53, GLB1, and CRYAA expression in ALCs from patients with ARC. (a) Immunoblotting of histone H3, p53, GLB1 and CRYAA in the lysate of ALCs with the nuclear grades are indicated. β-actin was used as the internal control. Densitometry analysis of (b) histone H3, (c) p53, (d) GLB1 and (e) CRYAA expression. Data were shown as mean ± SD and were analyzed using Kruskal-Wallis test with Dunn's post-hoc test. *, $p < 0.05$. ARC, age-related cataracts; ALC, anterior lens capsules; GLB1, β-galactosidase; CRYAA, αA-crystallin.

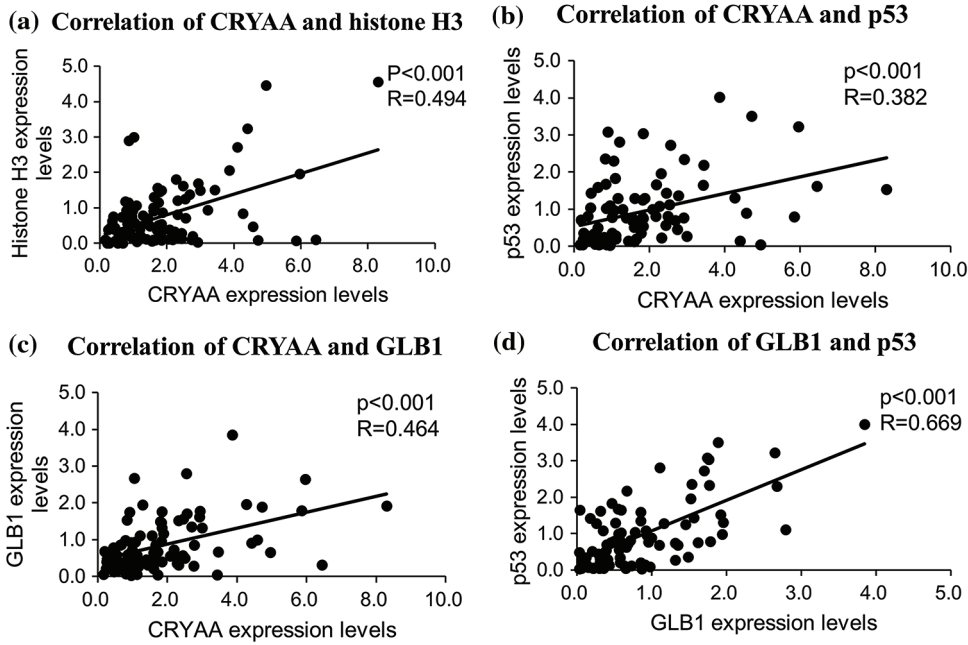


FIGURE 3. Correlation analysis of the results of immunoblotting. (a) The levels of CRYAA and histone H3 were positively correlated ($p < 0.001$). (b) The levels of p53 and CRYAA were positively correlated ($p < 0.001$). (c) The levels of GLB1 and CRYAA were positively correlated ($p < 0.001$). (d) The levels of GLB1 and p53 were positively correlated ($p < 0.001$). ARC, age-related cataracts; ALC, anterior lens capsules; GLB1, β -galactosidase; CRYAA, α A-crystallin. Data were analyzed using Pearson's correlation.

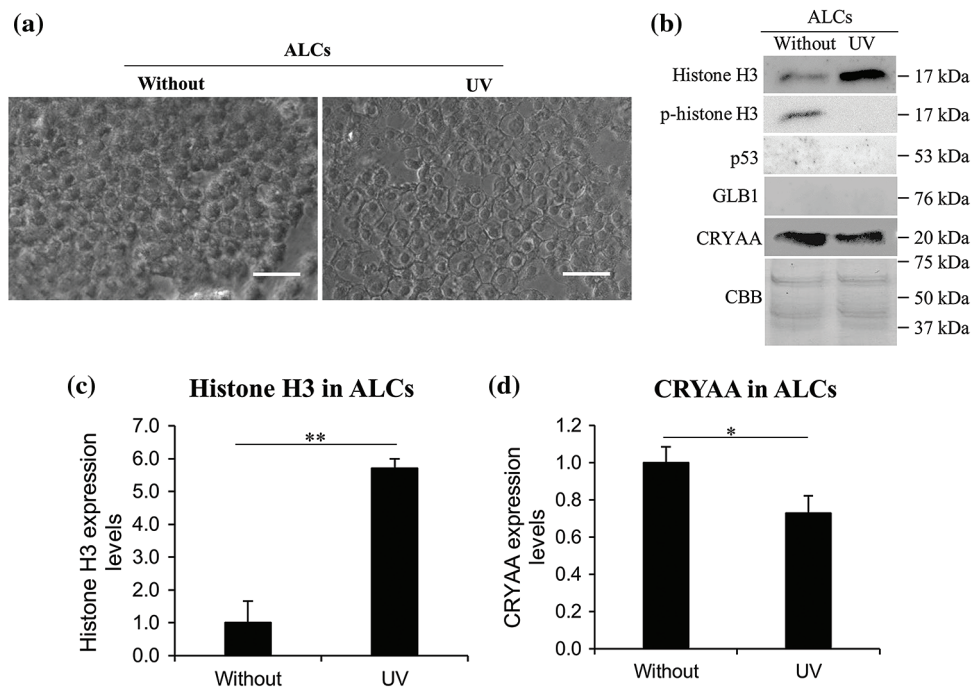


FIGURE 4. Histone H3, p-histone H3, p53, GLB1, and CRYAA in lysate of ALCs treated with UV irradiation. (a) Human lens epithelial cells in UV-treated and untreated ALCs of grade 2. Magnification, $\times 200$. (b) Detection of histone H3, p-histone H3, p53, GLB1 and CRYAA in UV-treated and untreated ALCs by IB. Coomassie brilliant blue staining was used to ensure equivalent loading. Densitometry analysis of (c) histone H3 and (d) CRYAA expression. Data were shown as mean \pm SD of at least three independent experiments. One-way ANOVA was performed with calculation of Tukey's Honest Significant Difference test to make pairwise comparisons within each experiment. *, $p < 0.05$; **, $p < 0.001$; ALC, anterior lens capsules; GLB1, β -galactosidase; CRYAA, α A-crystallin.

irradiation, SRA01/04 cells showed significantly increased mRNA levels of IL-6 ($p < 0.05$; Fig. 5d) and TNF- α ($p < 0.05$; Fig. 5e). Compared with the untreated SRA01/04 cells, UV-treated SRA01/04 cells showed higher levels of histone H3, GLB1, and CRYAA, and lower levels of p53 in the supernatant (Fig. 5f). IB results further showed lower expression levels of p53 ($p < 0.001$; Figs. 5f and 5g), GLB1 ($p < 0.001$; Figs. 5f and 5h) and CRYAA ($p < 0.001$; Figs. 5f and 5i), higher expression levels of p-histone H3

($p < 0.001$) (Figs. 5f and 5j) in lysate, and higher expression levels of histone H3 ($p < 0.05$; Figs. 5f and 5k) and p-histone H3 ($p < 0.001$) (Figs. 5c and 5l), and lower expression levels of p53 (Fig. 5f), GLB1 ($p < 0.05$; Figs. 5f and 5m) and CRYAA (Fig. 5f) in the BM. Compared with the untreated SRA01/04 cells, UV treated SRA01/04 cells showed significantly higher mRNA expression of histone H3 ($p < 0.001$; Fig. 5n), p53 ($p < 0.05$; Fig. 5o), CRYAA ($p < 0.05$; Fig. 5p), and p21 ($p < 0.001$; Fig. 5q).

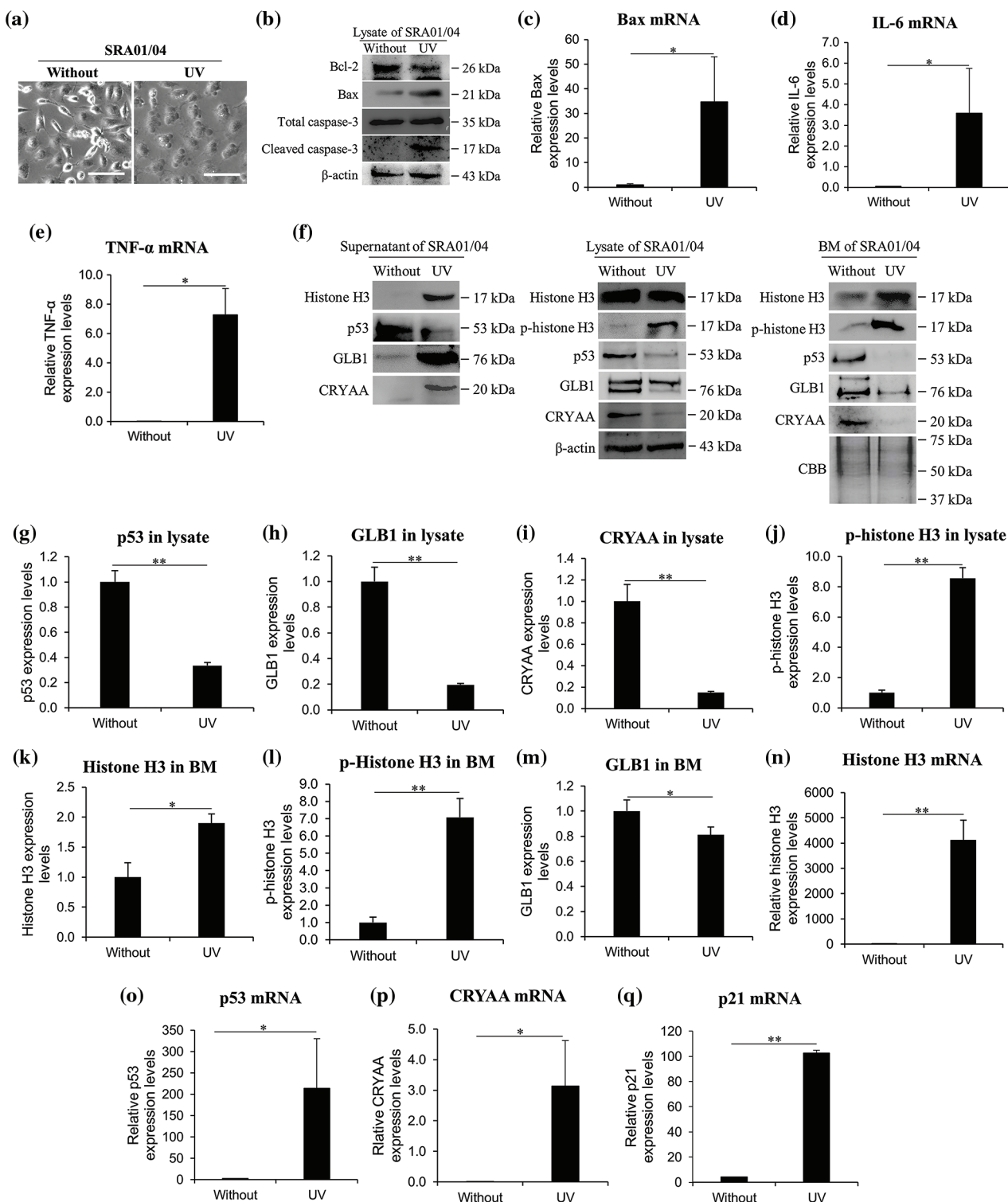


FIGURE 5. Apoptosis-related factors, histone H3, p-histone H3, p53, GLB1, and CRYAA expression in supernatant (PBS), lysate and BM of SRA01/04 cells treated by UV irradiation. (a) UV-treated and untreated SRA01/04. Magnification, $\times 200$. (b) Detection of apoptosis-related factors by IB. Detection of (c) Bax, (d) IL-6, and (e) TNF- α mRNA expression. (f) Detection of histone H3, p-histone H3, p53, GLB1, and CRYAA in UV-treated and untreated SRA01/04 cells by IB. β -actin was used as the loading control for cell lysate, Coomassie brilliant blue staining was used to ensure equivalent loading of the BM. Densitometry analysis of (g) p53, (h) GLB1, (i) CRYAA, and (j) p-histone H3 in the cell lysate, and of (k) histone H3, (l) p-histone H3, and (m) GLB1 in the BM. mRNA expression of (n) histone H3, (o) p53, (p) CRYAA, and (q) p21. Data are shown as mean \pm SD of at least three independent experiments. One-way ANOVA was performed with calculation of Tukey's Honest Significant Difference test to make pairwise comparisons within each experiment. *, $p < 0.05$, **, $p < 0.001$. BM, basement membrane; CRYAA, α A-crystallin; GLB1, β -galactosidase; IB, immunoblotting; IL-6, interleukin; UV, ultraviolet.

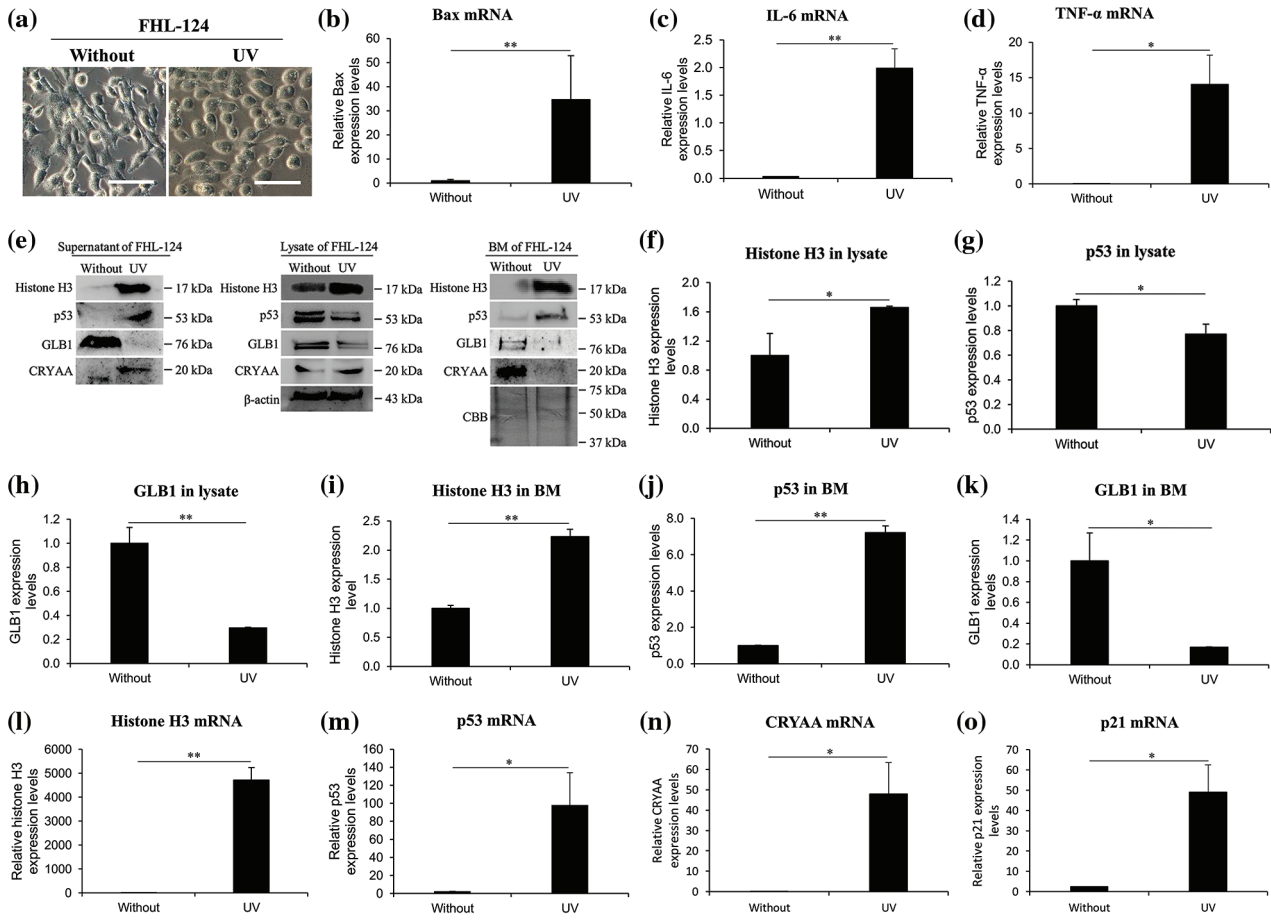


FIGURE 6. Histone H3, p53, GLB1 and CRYAA in supernatant (PBS), lysate and BM of FHL-124 cells treated with UV irradiation. (a) UV-treated (UV) and untreated (without) FHL-124. Magnification, $\times 200$. mRNA levels of (b) Bax, (c) IL-6 and (d) TNF- α . (e) Detection of histone H3, p53, GLB1 and CRYAA in UV-treated and untreated FHL-124 cells by IB. β -actin was used as the loading control for cell lysate, and Coomassie brilliant blue staining was used to ensure equivalent loading for the BM. Densitometry analysis of analysis of (f) histone H3, (g) p53 and (h) GLB1 in cell lysate, and of (i) histone H3, (j) p53 and (k) GLB1 in cell BM. (l–o) mRNA levels of (l) histone H3, (m) p53, (n) CRYAA and (o) p21. Data were shown as mean \pm SD of at least three independent experiments. One-way ANOVA was performed with calculation of Tukey's Honest Significant Difference test to make pairwise comparisons within each experiment. *, $p < 0.05$, **, $p < 0.001$. BM, basement membrane; CRYAA, α A-crystallin; GLB1, β -galactosidase; IB, immunoblotting; UV, ultraviolet.

Histone H3, p-histone H3, p53, β -galactosidase, and α A-crystallin expression in the supernatant, lysate, and basement membrane of FHL-124 cells treated with UV irradiation

In FHL-124 cells treated with UV irradiation as a model of ARC, the supernatant, lysate, and BM of FHL-124 cells were harvested and analyzed by IB for histone H3, p53, GLB1, and CRYAA expression. Total RNA was collected, and the mRNA expression of Bcl-2, Bax, IL-6, TNF- α , histone H3, p53, CRYAA, and p21 were detected. After UV irradiation, FHL-124 cells became swollen (Fig. 6a), and UV-induced cell apoptosis was further confirmed by the increased mRNA levels of Bax ($p < 0.001$; Fig. 6b). In addition, the mRNA expression levels of IL-6 ($p < 0.001$; Fig. 6c) and TNF- α ($p < 0.05$; Fig. 6d) were upregulated by UV irradiation. The mRNA expression levels of Bcl-2 were not altered (data not shown). Compared with the untreated FHL-124 cells, UV-treated cells showed higher expression levels of histone H3, p53, and CRYAA, and lower expression levels of GLB1 in the supernatant (Fig. 6e). The lysate of UV-treated cells showed higher expression levels of histone H3 ($p < 0.05$; Figs. 6e and 6f), lower expression levels of p53 ($p < 0.05$; Figs. 6e and 6g) and GLB1 ($p < 0.001$; Figs. 6e and 6h) in the lysate (Fig. 6e),

while the BM of these cells showed higher expression levels of histone H3 ($p < 0.001$; Figs. 6e and 6i) and p53 ($p < 0.001$; Figs. 6e and 6j), and lower expression levels of GLB1 (Figs. 6e and 6k; $p < 0.05$) and CRYAA (Fig. 6e). The p-histone H3 was not detectable in the supernatant, lysate, and BM of both UV treated and untreated FHL-124 cells (data not shown). Compared with the untreated FHL-124 cells, UV-treated cells showed significantly higher mRNA expression levels of histone H3 ($p < 0.001$, Fig. 6l), p53 ($p < 0.05$; Fig. 6m), CRYAA ($p < 0.05$; Fig. 6n), and p21 ($p < 0.05$; Fig. 6o).

α A-crystallin overexpression upregulates histone H3 in human lens epithelial cells

To study the effect of CRYAA overexpression on histone H3, p-histone H3, p53, and GLB1 levels in human lens epithelial cells, a CRYAA overexpression plasmid was transfected into SRA01/04 cells, and FHL-124 cells. The CRYAA transfected SRA01/04 cells showed higher mRNA expression of CRYAA, compared with the blank vector (Fig. 7a). The supernatant, lysate, and BM of these transfected cells showed similar expression of CRYAA and other assessed proteins (Fig. 7c). In the FHL-124 cells, compared with cells transfected with an empty vector, CRYAA

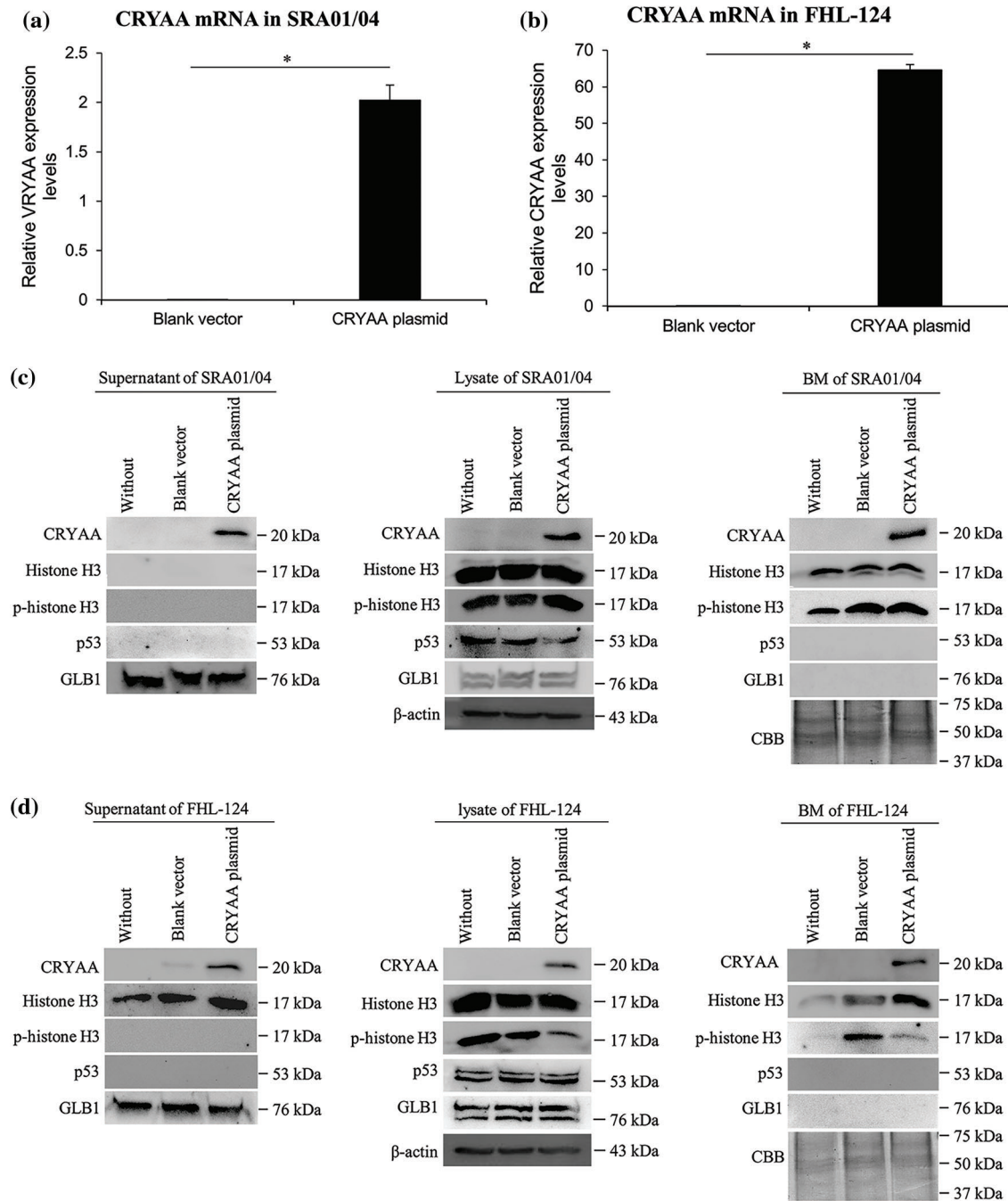


FIGURE 7. CRYAA overexpression upregulates histone H3 expression in human lens epithelial cells. Expression levels of CRYAA, histone H3, p-histone H3, p53, and GLB1 were detected in SRA01/04 cells and FHL-124 cells which were transfected with nothing (without), a blank vector (blank vector) or a CRYAA overexpression plasmid (CRYAA plasmid). (a and b) mRNA expression of CRYAA in (a) SRA01/04 cells and (b) FHL-124 cells. Data are shown as mean \pm SD of at least three independent experiments. One-way ANOVA was performed with calculation of Tukey's Honest Significant Difference test to make pairwise comparisons within each experiment. **, $p < 0.001$. IB detection of CRYAA, histone H3, p-histone H3, p53, and GLB1 in the supernatant, lysate, and BM of (c) SRA01/04 cells and (d) FHL-124 cells transfected with CRYAA plasmid. β -actin was used as the loading control for cell lysate, and Coomassie brilliant blue staining was used to ensure equivalent loading for the BM. CRYAA, α -crystallin; GLB1, β -galactosidase; BM, basement membrane.

plasmid transfection showed higher mRNA (Fig. 7b) and protein expression of CRYAA in the supernatant, lysate, and BM, a higher expression of histone H3 in the supernatant and BM, but lower expression of p-histone H3 in lysate and BM (Fig. 7d).

Discussion

In the present study, the expression levels of histone H3 and p53 in ALCs of ARC patients increased with nuclear grade,

suggesting that histone H3 and p53 might be involved in the development of ARC. To the best of our knowledge, this is the first report of abnormal expression of histone H3 in ARC. The expression of CRYAA was positively correlated with those of histone H3, p53, and GLB1 in ALCs of patients with ARC, indicating a regulatory relationship between the expression of CRYAA and histone H3, p53, or GLB1 in the pathogenesis of ARC. A potential limitation of this study was that immunohistochemistry of these factors

was not used. To further study the possible involvement of histone H3, CRYAA, p53, and GLB1 in the pathogenesis of ARC, a UV-treated ALC tissue model, and two cell models were utilized.

Cell apoptosis and cell senescence of human lens epithelial cells are both involved in the development of ARC (Li *et al.*, 1995; Fu *et al.*, 2016). ARC was originally considered a non-inflammatory condition; however, compared with the aqueous humor of children, the aqueous humor of patients with ARC showed increased concentrations of pro-inflammatory cytokines (Zheng *et al.*, 2018). UV light is implicated in the development of cataract (Zhu *et al.*, 2015), and several *in vivo* models, such as rabbit (Pitts *et al.*, 1977), rat (Merriam *et al.*, 2000), and human lens epithelial cells (Andley and Weber, 1995) have shown that UV irradiation could cause lens or cell damage. The present study is the first to report treatment of ALC tissues with UV irradiation to establish an *ex vivo* model of ARC, and this model may fill the gap between samples of ARC and models of human lens epithelial cells. The morphological aberrations of human lens epithelial cells in ALC tissues showed the efficacy of UV irradiation. In addition, UV irradiation resulted in changes in the expression of apoptosis-related (Bax, Bcl-2, and caspase-3), senescence-related (p53 and p21), and inflammation-related (TNF- α and IL-6) molecules in both SRA01/04 cells and FHL-124 cells, suggesting that the ARC cell models were also well established and representative.

The expression level of histone H3 was positively correlated with the nuclear grade of ARC. Changes in H3 expression may be induced by UV irradiation; to determine this, UV irradiated models of ALCs, and human lens epithelial cells were created, and the mRNA and the expression of histone H3 protein were assessed. Histone H3 upregulation was observed in UV-treated ALC tissues, cell supernatant, and BM of UV-treated SRA01/04 cells and in the cell supernatant, lysate, and BM of UV-treated FHL-124 cells. The increased mRNA expression of Histone H3 was also observed in UV-treated SRA01/04 and FHL-124 cells. The expression of p-histone H3 was analyzed and shown to increase in the lysate and BM of UV-treated SRA01/04 cells but decreased in UV-treated ALC tissues. These results further support the hypothesis that histone H3 upregulation may be involved in the pathogenesis of ARC; however, based on the current data, it is difficult to conclude whether p-histone H3 was also involved. Histone H3 may cause cell apoptosis in a dose-dependent manner by increasing Bax/Bcl-2, caspase-3, and caspase-9 expression or by perturbing calcium homeostasis, inducing the dysregulation of the unfolded protein response and increasing mitochondrial toxicity (Barrero *et al.*, 2013; Kawano *et al.*, 2014; Ibañez-Cabellos *et al.*, 2018). Endogenous histones may induce expressions of TNF- α and IL-6 (Chen *et al.*, 2014); therefore, histone H3 might participate in the pathogenesis of ARC via induction of cell apoptosis and inflammation. Accumulation of histone H3 in lens epithelial cells caused by UV or other stress increased with age. Histone H3 also induced apoptosis and inflammation, which aggravated nuclear opacity levels up to grade 4+, which may explain the increased expression of histone H3 in grade 4+ patients compared with patients with grades 2 ARC.

The expression of p53 was positively correlated with the nuclear grade of ARC. Overexpression of p53 was only

observed in PBS supernatant and BM of UV-treated FHL-124 cells; however, increased mRNA levels of p53 were observed in both UV-treated SRA01/04 and FHL-124 cells. The PBS supernatant of cells was concentrated in the present study, which may result in the detectable p53 expression levels in cells. However, the reason for relatively higher p53 expression levels in the cell supernatant of untreated SRA01/04 cells than that in treated cells is currently unknown. These results support the notion that UV irradiation may result in the upregulation of p53 expression. p53 has been previously detected in ALCs of ARC and may be induced by UV irradiation (Galichanin, 2017; Ayala *et al.*, 2007) or oxidative stress (Lu *et al.*, 2018). p53 has both proapoptotic and antiapoptotic functions (McKay *et al.*, 2000) and UV may result in DNA damage in the cells, which subsequently activates p53 to induce arrest of DNA repair through the upregulation of p21. The mRNA levels of p21 were upregulated by UV in the present study, providing additional support for this hypothesis. Upregulation of p53 is observed in cells a few hours after UV irradiation (McKay *et al.*, 2000). However, in the present study, the cell supernatant, lysate, and BM were collected immediately after UV irradiation. This may explain the relatively low levels of p53 protein expression in the cell lysate of FHL-124 cells and SRA01/04 cells in the UV group. The rapid harvest of various samples from tissues and cells after UV irradiation may have led to a failure in the detection of p53 upregulation. Thus, in future studies, the duration between UV irradiation and subsequent harvest should be longer. Nonetheless, the present study, for the first time, showed a positive correlation between p53 expression and the nuclear grades of ARC.

GLB1 is considered a senescence marker (Xing *et al.*, 2018) and might be related to p16 (Wagner *et al.*, 2015). In ALCs of ARC, GLB1 positive cells were detectable (Fu *et al.*, 2016). In the present study, expression levels of GLB1 in ALCs of ARC did not increase significantly with the nuclear grade of ARC, and GLB1 overexpression was only found in the supernatant of UV-treated SRA01/04 cells, suggesting that GLB1 may not be important for the development of ARC. However, considering the importance of p53 and its positive correlation with GLB1 in ALCs, the possible involvement of GLB1 in the pathogenesis of ARC should not be excluded, and perhaps a longer period of the gap between UV radiation and subsequent experimentation may show expression changes in GLB1, similar to that with p53.

Downregulation and mutations of CRYAA in lens epithelial cells could induce congenital cataract (Yang *et al.*, 2016; Khoshaman *et al.*, 2017). In the present study, the expression of CRYAA was positively correlated with histone H3, p53, and GLB1 in ALCs of ARC. Increased expression of CRYAA was observed in the supernatants of both UV-treated SRA01/04 and FHL-124 cells. Additionally, increased mRNA levels of CRYAA were also detected in both UV-treated SRA01/04 and FHL-124 cells. Following overexpression of CRYAA, although histone H3 levels were not significantly altered in cells, histone H3 protein levels were notably upregulated in the supernatant and BM of FHL-124 cells, suggesting that total histone H3 expression was upregulated and secreted out of the cells. Therefore, it is hypothesized that overexpression of CRYAA may upregulate histone H3

expression. These results suggest that CRYAA upregulation may be involved in the pathogenesis of ARC, possibly through the upregulation of histone H3. CRYAA overexpression resulted in increased levels of histone H3 but did not increase p53 and GLB1 expression, suggesting that p53 and GLB1 upregulation in ALCs of higher nuclear grades may not be induced by CRYAA and histone H3. Our recently published paper reported that CRYAA overexpression could promote corneal neovascularization (Yu *et al.*, 2019). Together, these results suggest that CRYAA may be an important molecule involved in the pathogenesis of eye diseases, in addition to its physiological role in lens development.

In conclusion, upregulation of histone H3 by CRYAA might be involved in the pathogenesis of ARC, and p53 may participate in ARC development, but not through the CRYAA-histone H3 axis.

Availability of Data and Materials: The analyzed data sets generated during the study are available from the corresponding author on reasonable request.

Author Contributions: PL, XLT, XGL, and HQ designed this study. XGL and HQ guided and supervised this study. CW, JWW, FQS, LYS, HRL, XW, ZT, XGL, and HQ collected samples and performed the experiments, data analysis, and interpretation. CW, XGL, and HQ wrote the manuscript. PL, WHZ, and XLT revised the manuscript. All authors checked and approved the manuscript.

Ethics Approval: All experiments were performed with the approval of the Internal Review Board of Harbin Medical University (Nos. 2021IIT028, 20210421) and were conducted in accordance with the Declaration of Helsinki Principles. Informed consent were obtained from all patients.

Consent for Publication: Written informed consent was obtained for all patients.

Funding Statement: This work was supported by the Nature Science Foundation of China (81470618); the Scientific Research Foundation of First Affiliated Hospital of Harbin Medical University (2017B013).

Conflicts of Interest: The authors declare that they have no competing interests.

References

- Andjelic S, Drašlar K, Hvala A, Hawlina M (2017). Anterior lens epithelium in cataract patients with retinitis pigmentosa-scanning and transmission electron microscopy study. *Acta Ophthalmologica* **95**: e212–e220. DOI 10.1111/aos.13250.
- Andley UP, Weber JG (1995). Ultraviolet action spectra for photobiological effects in cultured human lens epithelial cells. *Photochemistry and Photobiology* **62**: 840–846. DOI 10.1111/j.1751-1097.1995.tb09145.x.
- Ayala M, Strid H, Jacobsson U, Söderberg PG (2007). p53 expression and apoptosis in the lens after ultraviolet radiation exposure. *Investigative Ophthalmology & Visual Science* **48**: 4187–4191. DOI 10.1167/iovs.06-0660.
- Barrero CA, Perez-Leal O, Aksoy M, Moncada C, Ji R *et al.* (2013). Histone 3.3 participates in a self-sustaining cascade of apoptosis that contributes to the progression of chronic obstructive pulmonary disease. *American Journal of Respiratory and Critical Care Medicine* **188**: 673–683. DOI 10.1164/rccm.201302-0342OC.
- Beebe DC, Holekamp NM, Shui YB (2010). Oxidative damage and the prevention of age-related cataracts. *Ophthalmic Research* **44**: 155–165. DOI 10.1159/000316481.
- Chen R, Kang R, Fan XG, Tang D (2014). Release and activity of histone in diseases. *Cell Death & Disease* **5**: e1370. DOI 10.1038/cddis.2014.337.
- Flaxman SR, Bourne RRA, Resnikoff S, Ackland P, Braithwaite T *et al.* (2017). Vision loss expert group of the global burden of disease study, global causes of blindness and distance vision impairment 1990–2020: A systematic review and meta-analysis *The Lancet. Global Health* **5**: e1221–e1234. DOI 10.1016/S2214-109X(17)30393-5.
- Fu Q, Qin Z, Yu J, Yu Y, Tang Q, Lyu D, Zhang L, Chen Z, Yao K (2016). Effects of senescent lens epithelial cells on the severity of age-related cortical cataract in humans: A case-control study. *Medicine* **95**: e3869. DOI 10.1097/MD.0000000000003869.
- Galichanin K (2017). Exposure to subthreshold dose of UVR-B induces apoptosis in the lens epithelial cells and does not in the lens cortical fibre cells. *Acta Ophthalmologica* **95**: 834–838. DOI 10.1111/aos.13370.
- Hammond CJ, Snieder H, Spector TD, Gilbert CE (2000). Genetic and environmental factors in age-related nuclear cataracts in monozygotic and dizygotic twins. *The New England Journal of Medicine* **342**: 1786–1790. DOI 10.1056/NEJM200006153422404.
- Ibañez-Cabellos JS, Aguado C, Pérez-Cremades D, García-Giménez JL, Bueno-Betí C, García-López EM, Romá-Mateo C, Novella S, Hermenegildo C, Pallardó FV (2018). Extracellular histones activate autophagy and apoptosis via mTOR signaling in human endothelial cells. *Biochimica et Biophysica Acta (BBA)—Molecular Basis of Disease* **1864**: 3234–3246. DOI 10.1016/j.bbadis.2018.07.010.
- Ikeda T, Minami M, Nakamura K, Kida T, Fukumoto M, Sato T, Ishizaki E (2014). Progression of nuclear sclerosis based on changes in refractive values after lens-sparing vitrectomy in proliferative diabetic retinopathy. *Clinical Ophthalmology* **8**: 959–963. DOI 10.2147/OPHTH.S61372.
- Jin X, Jin H, Shi Y, Guo Y, Zhang H (2017). Long non-coding RNA KCNQ1OT1 promotes cataractogenesis via miR-214 and activation of the caspase-1 pathway. *Cellular Physiology and Biochemistry* **42**: 295–305. DOI 10.1159/000477330.
- Kawano H, Ito T, Yamada S, Hashiguchi T, Maruyama I, Hisatomi T, Nakamura M, Sakamoto T (2014). Toxic effects of extracellular histones and their neutralization by vitreous in retinal detachment. *Laboratory Investigation* **94**: 569–585. DOI 10.1038/labinvest.2014.46.
- Khairallah M, Kahloun R, Bourne R, Limburg H, Flaxman SR *et al.* (2015). Number of people blind or visually impaired by cataract worldwide and in world regions, 1990 to 2010. *Investigative Ophthalmology & Visual Science* **56**: 6762–6769. DOI 10.1167/iovs.15-17201.
- Khoshaman K, Yousefi R, Tamaddon AM, Abolmaali SS, Oryan A, Moosavi-Movahedi AA, Kurganov BI (2017). The impact of different mutations at Arg54 on structure, chaperone-like activity and oligomerization state of human α A-crystallin: The pathomechanism underlying congenital cataract-causing mutations R54L, R54P and R54C. *Biochimica et Biophysica Acta. Proteins and Proteomics* **1865**: 604–618. DOI 10.1016/j.bbapap.2017.02.003.

- Klein BE, Klein R, Lee KE (2002). Incidence of age-related cataract over a 10-year interval: The beaver dam eye study. *Ophthalmology* **109**: 2052–2057. DOI 10.1016/S0161-6420(02)01249-6.
- Li WC, Kuszak JR, Dunn K, Wang RR, Ma W, Wang GM, Spector A, Leib M, Cotliar AM, Weiss M (1995). Lens epithelial cell apoptosis appears to be a common cellular basis for non-congenital cataract development in humans and animals. *The Journal of cell biology* **130**: 169–181. DOI 10.1083/jcb.130.1.169.
- Lu B, Christensen IT, Ma LW, Wang XL, Jiang LF, Wang CX, Feng L, Zhang JS, Yan QC (2018). miR-24-p53 pathway evoked by oxidative stress promotes lens epithelial cell apoptosis in age-related cataracts. *Molecular Medicine Reports* **17**: 5021–5028. DOI 10.3892/mmr.2018.8492.
- McKay BC, Chen F, Perumalswami CR, Zhang F, Ljungman M (2000). The tumor suppressor p53 can both stimulate and inhibit ultraviolet light-induced apoptosis. *Molecular Biology of the Cell* **11**: 2543–2551. DOI 10.1091/mbc.11.8.2543.
- Merriam JC, Löfgren S, Michael R, Söderberg P, Dillon J, Zheng L, Ayala M (2000). An action spectrum for UV-B radiation and the rat lens. *Investigative Ophthalmology & Visual Science* **41**: 2642–2647.
- Nizami AA, Gulani AC (2021). Cataract. In: *StatPearls*. Treasure Island (FL): StatPearls Publishing.
- Pitts DG, Cullen AP, Hacker PD (1977). Ocular effects of ultraviolet radiation from 295 to 365 nm. *Investigative Ophthalmology & Visual Science* **16**: 932–939.
- Richard AH (2019). Lens. In: Paul RE, James JA, (eds.), *Vaughan & Asbury's General Ophthalmology (19e)*, pp. 398–415. New York: McGraw-Hill Education Inc.
- Tang Y, Wang X, Wang J, Huang W, Gao Y, Luo Y, Yang J, Lu Y (2016). Prevalence of age-related cataract and cataract surgery in a Chinese adult population: The Taizhou eye study. *Investigative Ophthalmology & Visual Science* **57**: 1193–1200. DOI 10.1167/iovs.15-18380.
- Thompson J, Lakhani N (2015). Cataracts. *Primary Care* **42**: 409–423. DOI 10.1016/j.pop.2015.05.012.
- Truscott RJ (2005). Age-related nuclear cataract-oxidation is the key. *Experimental Eye Research* **80**: 709–725. DOI 10.1016/j.exer.2004.12.007.
- Vinson JA (2006). Oxidative stress in cataracts. *Pathophysiology* **13**: 151–162. DOI 10.1016/j.pathophys.2006.05.006.
- Wagner J, Damaschke N, Yang B, Truong M, Guenther C, McCormick J, Huang W, Jarrard D (2015). Overexpression of the novel senescence marker β -galactosidase (GLB1) in prostate cancer predicts reduced PSA recurrence. *PLoS One* **10**: e0124366. DOI 10.1371/journal.pone.0124366.
- Xing J, Ying Y, Mao C, Liu Y, Wang T, Zhao Q, Zhang X, Yan F, Zhang H (2018). Hypoxia induces senescence of bone marrow mesenchymal stem cells via altered gut microbiota. *Nature Communications* **9**: 2020. DOI 10.1038/s41467-018-04453-9.
- Yan Y, Qian H, Jiang H, Yu H, Sun L et al. (2018). Laminins in an *in vitro* anterior lens capsule model established using HLE B-3 cells. *Molecular Medicine Reports* **17**: 5726–5733. DOI 10.3892/mmr.2018.8581.
- Yan Y, Yu H, Sun L, Liu H, Wang C et al. (2019). Laminin α 4 overexpression in the anterior lens capsule may contribute to the senescence of human lens epithelial cells in age-related cataract. *Sedentary Life and Nutrition* **11**: 2699–2723. DOI 10.18632/aging.101943.
- Yang J, Zhou S, Guo M, Li Y, Gu J (2016). Different alpha crystallin expression in human age-related and congenital cataract lens epithelium. *BMC Ophthalmology* **16**: 67. DOI 10.1186/s12886-016-0241-1.
- Yao K, Zhang L, Zhang Y, Ye P, Zhu N (2008). The flavonoid, fisetin, inhibits UV radiation-induced oxidative stress and the activation of NF-kappaB and MAPK signaling in human lens epithelial cells. *Molecular Vision* **14**: 1865–1871.
- Yu H, Sun L, Cui J, Li Y, Yan Y et al. (2019). Three kinds of corneal host cells contribute differently to corneal neovascularization. *EBioMedicine* **44**: 542–553. DOI 10.1016/j.ebiom.2019.05.026.
- Zeng M, Liu X, Liu Y, Xia Y, Luo L, Yuan Z, Zeng Y, Liu Y (2008). Torsional ultrasound modality for hard nucleus phacoemulsification cataract extraction. *The British Journal of Ophthalmology* **92**: 1092–1096. DOI 10.1136/bjo.2007.128504.
- Zheng Y, Rao YQ, Li JK, Huang Y, Zhao P, Li J (2018). Age-related pro-inflammatory and pro-angiogenic changes in human aqueous humor. *International Journal of Ophthalmology* **11**: 196–200. DOI 10.18240/ijo.2018.02.03.
- Zhu M, Yu J, Gao Q, Wang Y, Hu L, Zheng Y, Wang F, Liu Y (2015). The relationship between disability-adjusted life years of cataracts and ambient erythemal ultraviolet radiation in China. *Journal of Epidemiology* **25**: 57–65. DOI 10.2188/jea.JE20140017.